J. Cent. South Univ. (2014) 21: 2935−2943
DOI: 10.1007/s11771-014-2260-5

Springer

New methods of safety evaluation for rock/soil mass surrounding tunnel under earthquake

CHENG Xuan-sheng(程选生)[1, 2, 3], DOWDING Charles H[2], TIAN Rui-rui(田瑞瑞)[1]

1. School of Civil Engineering, Lanzhou University of Technology, Lanzhou 730050, China;
2. Department of Civil and Environmental Engineering, Northwestern University, Evanston 60208, USA;
3. Key Laboratory of Urban Security and Disaster Engineering of Education Ministry, Beijing University of Technology, Beijing 100124, China

Abstract: The objective of this work is to obtain the seismic safety coefficient and fracture surface and proceed with the seismic safety evaluation for the rock mass or soil mass surrounding a tunnel, and the limitation of evaluating seismic stability is considered using the pseudo-static strength reduction. By using the finite element software ANSYS and the strength reduction method, new methods of seismic safety evaluation for the rock mass or soil mass surrounding a tunnel are put forward, such as the dynamic finite element static shear strength reduction method and dynamic finite element shear strength reduction method. In order to prove the feasibility of the proposed methods, the results of numerical examples are compared with that of the pseudo-static strength reduction method. The results show that 1) the two methods are both feasible, and the plastic zone first appears near the bottom corners; 2) the safety factor of new method II is smaller than that of new method I but generally, and the difference is very small. Therefore, in order to ensure the safety of the structure, two new methods are proposed to evaluate the seismic stability of the rock mass or soil mass surrounding a tunnel. A theoretical basis is provided for the seismic stability of the rock mass or soil mass and the lining surrounding a tunnel and also provided for the engineering application.

Key words: tunnel; rock or soil mass surrounding tunnel; earthquake stability; safety evaluation

1 Introduction

With the rapid development of transportation construction, various forms of tunnels have been widely used in railway, highway, urban underground engineering, water conservancy, mine construction and military and civil engineering. The safety of the rock mass or soil mass structure surrounding a tunnel should be not only associated with its geological characteristics but also with all sorts of natural factors, such as damage caused by earthquakes and environmental vibrations caused by volcanic eruptions and explosions. There were serious collapses of caves and tunnels during the 2008 Wenchuan earthquake and the 7.1 magnitude earthquake that happened on April 14, 2010 in Yushu County of the Tibetan autonomous prefecture of Qinghai Province in China. Hydropower engineering facilities were destroyed, and the railway and highway traffics were stopped and an incalculable economic loss of the property of the people and state was caused.

In China, many cities have been located in areas of high seismic intensity, and the seismic intensity is generally the 8th degree or more. Strong earthquakes have happened more than twice every three years and almost 50% of the earthquakes have caused serious damage [1]. Therefore, the safety assessment of tunnel ground motion is very important. When conducting a safety evaluation of a tunnel structure under earthquake, the safety assessment of the rock mass or soil mass structure surrounding a tunnel is firstly performed.

At present, because of the rapid development of technology and the extensive application of engineering, the stress analysis and static safety coefficient calculation of the tunnel structure have been done. The calculation method of the underground cavity safety coefficient was based on the principle strength reduction, as discussed by JIANG et al [2]. An analysis of the stability of the rock mass or soil mass surrounding a tunnel was performed using the method of the minimum safety coefficient [3]. The stability of a shallow tunnel was also analyzed [4−6]. The quasi-static and ground motion internal force of a loess cave was analyzed using the maximum tensile stress theory and the internal force of the tunnel lining

Foundation item: Project(2011CB013600) supported by State Key Program for Basic Research of China; Project(20136201110003) supported by the Education Ministry Doctoral Tutor Foundation of China; Project(51368039) supported by the National Natural Science Foundation of China; Project(2013-4-94) supported by the Program of Science and Technology Research in Lanzhou City, China
Received date: 2013−03−15; **Accepted date:** 2013−06−13
Corresponding author: CHENG Xuan-sheng, Professor, PhD; Tel: +86−931−2973784; E-mail: cxs702@126.com, Chengxuansheng@gmail.com

structure was also analyzed [7−8]. Considering a plane strain and three-dimensional problem, the time history analysis of a loess cave under various earthquakes was analyzed using maximum tensile stress theory [9]. The method of finite element strength reduction was also used in a tunnel and the tunnel static safety coefficient was also analyzed [10−15]. Meanwhile, based on the method of pseudo-static analysis, the earthquake reliability of an underground tunnel was also done [16].

For the method of pseudo-static strength reduction, the load and stability analysis method are both static. Its advantages are: the clear physical conception, the simple calculation method, the small computing workload and the easy determination of parameters. It is easy for design engineers to accept. Thus, the method is suitable for the seismic design of structures for small accelerations but not suitable for serious dynamic action. Present research results have laid a solid foundation for the evaluation of the ground motion safety of tunnel structures. Therefore, based on the existing literature, this work will consider the effect of horizontal earthquake and propose new methods of safety assessment of rock mass or soil mass surrounding a tunnel, such as dynamic finite element static shear strength reduction method and dynamic finite element shear strength reduction method. Thus, the theoretical basis for ground motion stability analysis and engineering application of rock mass or soil mass structure and lining structure surrounding a tunnel will be provided.

2 Pseudo-static reduction methods

The method is the simple acceleration or inertial force method. The basic idea is to simplify the earthquake effect as an additional inertial force system of the research object. It is a simple method using the static method to solve approximately the dynamical problem. According to intensity values of a given seismic action, load is generally taken as one-third or half of the average peak acceleration or directly, and then the safety coefficient is calculated using the static stability analysis method.

Because the safety of the engineering structure is paramount and due to the computational demands, the model size is fixed as five times tunnel span. According to Ref. [17], cutting an isolation body vertically along the loess tunnel, the upper boundary is taken to the surface. Boundary condition at the bottom is fixed hinge constraints, the upper side is free and the two sides of the border are horizontal constraints. As the tunnels longitudinal length is much larger than its cross-section, it is considered as a plane strain problem and the analysis model is shown in Fig. 1.

Through constantly discounting soil or rock mass shear strength parameters until instability damage occurs, the safety stability coefficient of the rock mass or soil mass surrounding a tunnel will be obtained by pseudo-static analysis of shear strength reduction method.

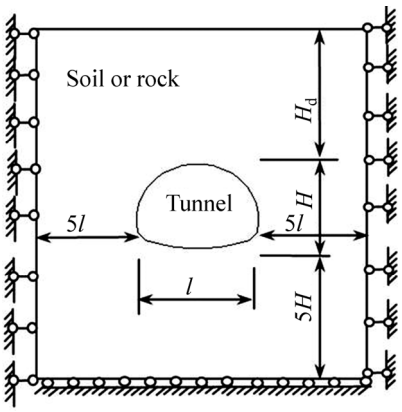

Fig. 1 Static analysis model

3 New methods

As stated above, the load determination and the stability analysis method are both static. Therefore, there are some limitations for earthquake safety evaluation and it is necessary to propose new methods of stability analysis.

3.1 New method I: Dynamic finite element static shear strength reduction method

3.1.1 Numerical modal analysis

In order to obtain the damping matrix of the finite element differential equation under earthquake, the modal analysis of structure isolation body should be dealt with first. Using the security coefficient calculation with 5 times, 10 times, 15 times and 20 times tunnel span, the engineering accuracy requirement can be satisfied with five times tunnel span. Therefore, it is the same as the pseudo-static strength reduction method; both the left and right sides are 5 times tunnel span. The upper boundary is taken to the surface. Boundary conditions at the bottom are fixed hinge constraints, the upper side is free and the two sides of the border are horizontal constraints. As the tunnel longitudinal length is much larger than its cross-section, it is also considered as a plane strain problem and the analysis model is shown in Fig. 2.

Because the Rayleigh damper is simple and convenient, it is chosen in the analysis. The damping matrix $\boldsymbol{C}$ of the isolated body is assumed as the combination of the quality matrix $\boldsymbol{M}$ and stiffness matrix $\boldsymbol{K}$ [18], namely:

$$\boldsymbol{C} = \alpha \boldsymbol{M} + \beta \boldsymbol{K} \tag{1}$$

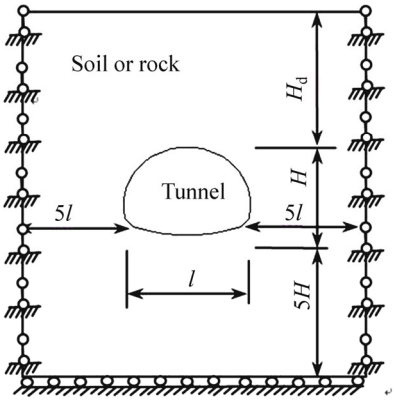

Fig. 2 Dynamic analysis model

where α is the mass damping coefficient and β is the stiffness damping coefficient. Both α and β are defined as follows:

$$\alpha=\frac{2\omega_i\omega_j}{\omega_i+\omega_j}\xi,\quad \beta=\frac{2}{\omega_i+\omega_j}\xi \tag{2}$$

where ξ is the damping ratio corresponding to the i-th or j-th vibration mode (similarly taking $\xi_i=\xi_j$, and can be obtained from experimental data); ω_i and ω_j are two different vibration circular frequencies.

3.1.2 Dynamic finite element theory analysis

The finite element matrix [18] of an isolated body under earthquake is as follows:

$$\boldsymbol{M}\ddot{\boldsymbol{u}}(t)+\boldsymbol{C}\dot{\boldsymbol{u}}(t)+\boldsymbol{K}\boldsymbol{u}(t)=-\boldsymbol{M}\ddot{\boldsymbol{u}}_{\boldsymbol{g}}(t) \tag{3}$$

where $\ddot{\boldsymbol{u}}(t)$, $\dot{\boldsymbol{u}}(t)$ and $\boldsymbol{u}(t)$ are the isolated body node acceleration vector, velocity vector and displacement vector, respectively; $\boldsymbol{M}$, $\boldsymbol{C}$ and $\boldsymbol{K}$ are the isolated body mass matrix, damping matrix and stiffness matrix, respectively. Equation (3) is solved by the Newmark integration method, namely:

$$\boldsymbol{u}_{t+\Delta t}=\boldsymbol{u}_t+\Delta t\dot{\boldsymbol{u}}_t+\left(\frac{1}{2}-\delta\right)\Delta t^2\ddot{\boldsymbol{u}}_t+\delta\Delta t^2\ddot{\boldsymbol{u}}_{t+\Delta t} \tag{4}$$

$$\dot{\boldsymbol{u}}_{t+\Delta t}=\dot{\boldsymbol{u}}_t+(1-\gamma)\Delta t\ddot{\boldsymbol{u}}_t+\gamma\Delta t\ddot{\boldsymbol{u}}_{t+\Delta t} \tag{5}$$

where γ and δ are both constants. At the moment of $t+\Delta t$, the motion differential equation is

$$\boldsymbol{M}\ddot{\boldsymbol{u}}_{t+\Delta t}+\boldsymbol{C}\dot{\boldsymbol{u}}_{t+\Delta t}+\boldsymbol{K}\boldsymbol{u}_{t+\Delta t}=-\boldsymbol{M}\ddot{\boldsymbol{u}}_{\boldsymbol{g}(t+\Delta t)} \tag{6}$$

Taking γ=1/2, δ=1/4 and $\Delta t\le\frac{T_{\max}}{100}$ ($T_{\max}$ is the biggest vibration period of the isolated body), the technique of the Newmark method is stability without any conditions and the precision of the result is satisfied.

Putting Eq. (4) and Eq. (5) into Eq. (6) gives

$$\left(\boldsymbol{M}+\frac{\Delta t}{2}\boldsymbol{C}\right)\ddot{\boldsymbol{u}}_{t+\Delta t}+\boldsymbol{C}\left(\dot{\boldsymbol{u}}_t+\frac{\Delta t}{2}\ddot{\boldsymbol{u}}_t\right)+\boldsymbol{K}\boldsymbol{u}_{t+\Delta t}=-\boldsymbol{M}\ddot{\boldsymbol{u}}_{\boldsymbol{g}(t+\Delta t)} \tag{7}$$

As known from Eq. (5), there is

$$\ddot{\boldsymbol{u}}_{t+\Delta t}=\frac{4}{\Delta t^2}\left(\boldsymbol{u}_{t+\Delta t}-\boldsymbol{u}_t\right)-\frac{4}{\Delta t}\dot{\boldsymbol{u}}_t-\ddot{\boldsymbol{u}}_t \tag{8}$$

Putting Eq. (8) into Eq. (7) produces

$$\left(\boldsymbol{K}+\frac{2}{\Delta t}\boldsymbol{C}+\frac{4}{\Delta t^2}\boldsymbol{M}\right)\boldsymbol{u}_{t+\Delta t}=\boldsymbol{C}\left(\frac{2}{\Delta t}\boldsymbol{u}_t+\dot{\boldsymbol{u}}_t\right)+\boldsymbol{M}\left(\frac{4}{\Delta t^2}\boldsymbol{u}_t+\frac{4}{\Delta t}\dot{\boldsymbol{u}}_t+\ddot{\boldsymbol{u}}_t\right)-\boldsymbol{M}\ddot{\boldsymbol{u}}_{\boldsymbol{g}(t+\Delta t)} \tag{9}$$

where $\boldsymbol{u}_{t+\Delta t}$ is obtained by Eq. (9); $\ddot{\boldsymbol{u}}_{t+\Delta t}$ and $\dot{\boldsymbol{u}}_{t+\Delta t}$ are obtained by Eq. (8) and Eq. (7), respectively.

Through the above solving, the moment T' of maximum horizontal displacement at vertex A can be obtained.

3.1.3 Seismic wave applied

In order to simulate the dynamic response of a tunnel structure under earthquake, an El-Centro wave is used for seismic response analysis. For simplicity, the seismic wave is input in the horizontal direction from the bottom. The El-Centro wave is shown in Fig. 3. The duration time is 10 s.

For the consideration of the influence of the seismic load to the isolation body safety coefficient of the rock mass or soil mass surrounding a tunnel, for $t\in[0,T']$, by repeating Eq. (4) to Eq. (9), the horizontal displacement

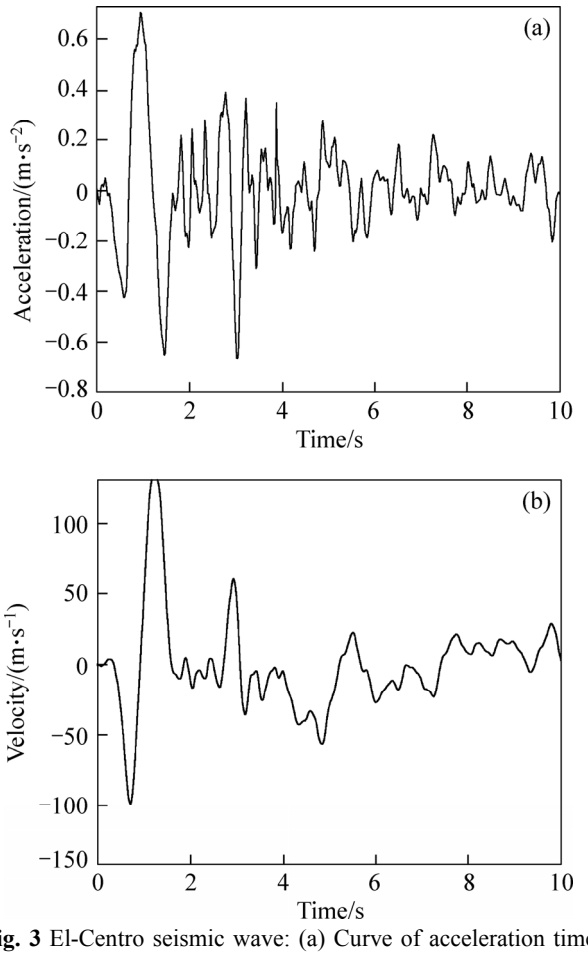

Fig. 3 El-Centro seismic wave: (a) Curve of acceleration time history; (b) Curve of velocity time history

on the vertical border of each node at the time of T' can be obtained.

After the dynamic analysis, importing the two side boundaries as in the pseudo-static analysis model and importing the horizontal displacement node by node, the strength parameters of the rock mass or soil mass surrounding a tunnel are reduced continuously until instability damage occurs. Thus, the structure stability safety coefficient of dynamic finite element static strength reduction analysis is obtained.

3.2 New method II: Dynamic finite element shear strength reduction method

3.2.1 Modal analysis and analysis model

Modal analysis is the same as method I. As known through the application of the pseudo-static strength reduction method and the dynamic finite element static shear strength reduction method, some local places of the internal rock/soil mass surrounding a tunnel are destroyed. In order to realize the dynamic finite element strength reduction method and lessen the influence of the rock/soil mass material strength reduction to seismic response and safety factor, the outer is viewed as an elastic zone and a certain thickness of rock mass or soil mass from inside is taken as the shear strength reduction area, so that the whole process of dynamic finite element shear strength reduction is realized. The two layers are set with the same material parameters. The analysis model is shown in Fig. 4.

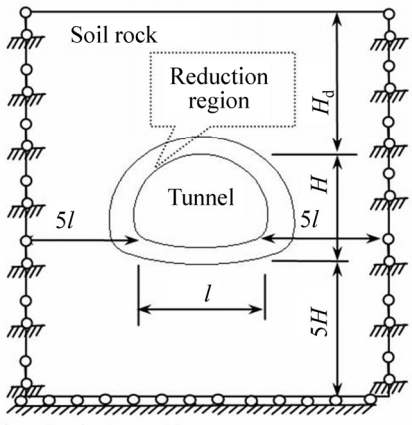

Fig. 4 Analysis model of new method II

3.2.2 Boundary conditions

The rock mass or soil mass surrounding a tunnel under gravity produces not only the counteracting force on the border but also the gravity stress inside the isolation body. Therefore, in order to realize the dynamic finite element shear strength reduction method, the counteracting force and the influence of gravity of the isolation body should be considered. The dynamic balance equation is obtained from the isolation body static equilibrium position, so the weight influence of the rock or soil mass surrounding a tunnel is not considered. The structure weight should be changed into an external load during the analysis.

1) Level counteracting force of vertical boundary

In order to determine each boundary counteracting force at the node of the structure isolation body dynamic analysis model under earthquake, the vertical constraints on both sides of the border in Fig. 4 is changed into horizontal constraints (shown in Fig. 5).

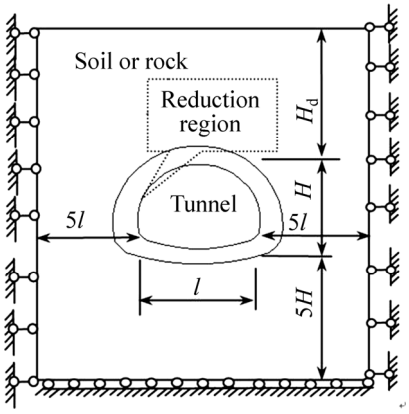

Fig. 5 Horizontal constraints of analysis model

Through the static finite element analysis, the horizontal border counteracting force of both sides can be determined.

2) Equivalent boundary conditions of gravity stress

According to the half space elastic model, the rock mass or soil mass surrounding a tunnel is supposed as a half infinite space linear deformation body. Therefore, the vertical gravity stress of homogeneous soil of each point at any level surface is a uniform distribution. It is also proportional to depth z and is a linear distribution along the depth, namely:

$$\sigma_{cz} = \rho g z \tag{10}$$

where ρ is the soil natural bulk density and z is the soil depth. As known from Hooke's law, there is

$$\sigma_0 = E\varepsilon_0 \tag{11}$$

As shown in Fig. 6, the temperature difference between the soil surface and the unit of vertical direction is ΔT and thus, the temperature deformation is

$$\varepsilon_0 = \alpha \Delta T z \tag{12}$$

where α is the linear expansion coefficient of material, and $\sigma_{cz}=\sigma_0$, as known from Eqs. (10), (11) and (12), there is

$$\Delta T = \frac{\rho g}{E\alpha} \tag{13}$$

Setting the temperature of the top boundary to zero, the temperature of the vertical and bottom boundaries can be obtained from Eq. (13). Then, the temperature

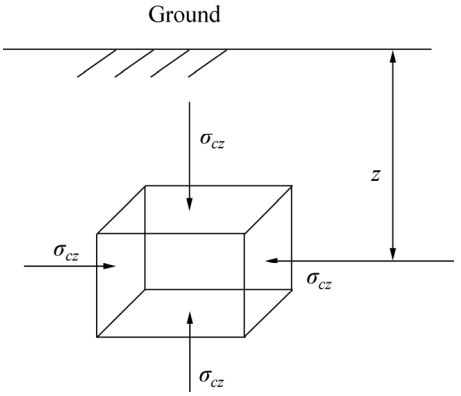

Fig. 6 Element gravity

difference obtained by Eq. (13) is put into Eq. (12), and the terms E and α both disappear according to Eq. (11) and Eq. (12). For the sake of simplicity, α is taken as 1. In order to obtain the temperature stress, the tunnel hole is viewed as a transition zone and the elastic modulus and Poisson ratio are set as 10^{-5} and the density is zero. The analysis model is shown as Fig. 7.

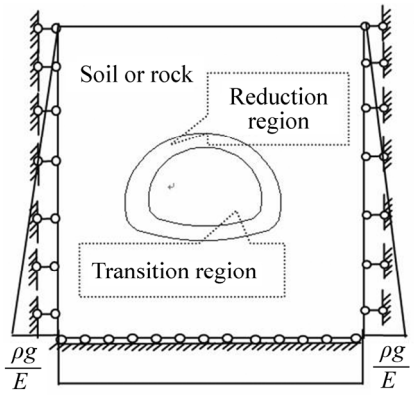

Fig. 7 Thermal analysis model

3.2.3 Dynamic finite element strength reduction method

The matrix differential equation of the isolation body under earthquake is as follows:

$$\boldsymbol{M}\ddot{\boldsymbol{u}}(t)+\boldsymbol{C}\dot{\boldsymbol{u}}(t)+\boldsymbol{K}\boldsymbol{u}(t)=-\boldsymbol{M}\ddot{\boldsymbol{u}}_{\boldsymbol{g}}(t)+\boldsymbol{P}_{\varepsilon_0}+\boldsymbol{P}_{\mathrm{f}} \tag{14}$$

where $\boldsymbol{P}_{\mathrm{f}}$ is the surface load vector; $\boldsymbol{P}_{\varepsilon_0}$ is the force vector caused by temperature strain.

$$\begin{cases}\boldsymbol{P}_{\varepsilon_0}=\sum\limits_{e}\int\limits_{\Omega_e}\boldsymbol{B}^{\mathrm{T}}\boldsymbol{D}\boldsymbol{\varepsilon}_0\mathrm{d}\Omega\\ \boldsymbol{\varepsilon}_0=\alpha(\boldsymbol{\varphi}-\boldsymbol{\varphi}_0)(1\quad 1\quad 0)^{\mathrm{T}}\end{cases}$$

where $\boldsymbol{D}$ is the elastic matrix; $\boldsymbol{B}$ is the strain matrix; $\boldsymbol{\varphi}$ is the temperature field vector; $\boldsymbol{\varphi}_0$ is the initial temperature field vector.

The Newmark method is adopted and $\boldsymbol{u}_{t+\Delta t}$ and $\dot{\boldsymbol{u}}_{t+\Delta t}$ are obtained from Eq. (4) and Eq. (5), respectively.

The motion differential equation at the time of $t+\Delta t$ is

$$\boldsymbol{M}\ddot{\boldsymbol{u}}_{t+\Delta t}+\boldsymbol{C}\dot{\boldsymbol{u}}_{t+\Delta t}+\boldsymbol{K}\boldsymbol{u}_{t+\Delta t}=-\boldsymbol{M}\ddot{\boldsymbol{u}}_{\boldsymbol{g}(t+\Delta t)}+\boldsymbol{P}_{\varepsilon_0}+\boldsymbol{P}_{\mathrm{f}} \tag{15}$$

Putting Eq. (4) and Eq. (5) into Eq. (17) gives

$$\left(\boldsymbol{M}+\frac{\Delta t}{2}\boldsymbol{C}\right)\ddot{\boldsymbol{u}}_{t+\Delta t}+\boldsymbol{C}\left(\dot{\boldsymbol{u}}_t+\frac{\Delta t}{2}\ddot{\boldsymbol{u}}_t\right)+\boldsymbol{K}\boldsymbol{u}_{t+\Delta t}=-\boldsymbol{M}\ddot{\boldsymbol{u}}_{\boldsymbol{g}(t+\Delta t)}+\boldsymbol{P}_{\varepsilon_0}+\boldsymbol{P}_{\mathrm{f}} \tag{16}$$

$\ddot{\boldsymbol{u}}_{t+\Delta t}$ is obtained by Eq. (5) and so

$$\left(\boldsymbol{K}+\frac{2}{\Delta t}\boldsymbol{C}+\frac{4}{\Delta t^2}\boldsymbol{M}\right)\boldsymbol{u}_{t+\Delta t}=\boldsymbol{C}\left(\frac{2}{\Delta t}\boldsymbol{u}_t+\dot{\boldsymbol{u}}_t\right)+\boldsymbol{M}\left(\frac{4}{\Delta t^2}\boldsymbol{u}_t+\frac{4}{\Delta t}\dot{\boldsymbol{u}}_t+\dot{\boldsymbol{u}}_t\right)-\boldsymbol{M}\ddot{\boldsymbol{u}}_{\boldsymbol{g}(t+\Delta t)}+\boldsymbol{P}_{\varepsilon_0}+\boldsymbol{P}_{\mathrm{f}} \tag{17}$$

Then, $\boldsymbol{u}_{t+\Delta t}$ is obtained by Eq. (17), and thus $\ddot{\boldsymbol{u}}_{t+\Delta t}$ and $\dot{\boldsymbol{u}}_{t+\Delta t}$ are derived.

The seismic wave is applied as in method I. Then, the strength parameters of the rock mass or soil mass surrounding a tunnel are reduced continuously until instability damage occurs, and thus the rock or soil mass stability safety coefficient of dynamic finite element strength reduction analysis is obtained.

4 Method of strength reduction and failure criterion

4.1 Method of strength reduction

The strength reduction [11, 19] is just reduced by $\boldsymbol{\eta}$ for the shear strength parameters c and $\tan\varphi$ of the soil mass or rock mass, respectively, until the limiting damage state is reached. According to the elastic-plastic finite element calculation results, the rock/soil failure face is obtained automatically by the program. Thus, the safety coefficient is just the reduction factor of rock mass or soil mass, namely:

$$c'=\frac{c}{\eta},\ \varphi'=\arctan\left(\frac{\tan\varphi}{\eta}\right) \tag{18}$$

and therefore,

$$\tau=\frac{c}{\eta}+\sigma\frac{\tan\varphi}{\eta}=c'+\sigma\tan\varphi' \tag{19}$$

4.2 Failure criterion

The rock mass or soil mass surrounding a tunnel is assumed as an ideal elastic-plastic material and the Mohr-Coulomb's failure criterion associated with plane strain is applied. The expression is

$$F=\lambda I_1+\sqrt{J_2}=k \tag{20}$$

where I_1 and J_2 are the first invariant of the stress tensor and the second invariant of the deviatoric stress tensor, respectively, and λ and k are the related constants for the cohesion c' and internal friction angle φ' of the

geological material. The expressions are

$$\lambda=\frac{\sin\varphi'}{\sqrt{3(3+\sin^2\varphi')}},\ k=\frac{3c'\cos\varphi'}{\sqrt{3(3+\sin^2\varphi')}} \tag{21}$$

5 Numerical examples

5.1 Calculation parameters and grid meshing

To facilitate convenient analysis, the soil mass is taken as the research object. The material parameters of the soil mass surrounding a tunnel are listed in Table 1 [8]. It is viewed as an elastic-plastic material, the loess tunnel span is 6 m and the covering soil thickness is 8 m and bears the 8th degree seismic precautionary intensity. Then, the safety factor of the tunnel structure under earthquake is obtained. The acceleration schedule curve maximum value is 0.70 m/s^2.

Table 1 Material parameters of soil mass

Modulus elasticity/MPa	Poisson ratio, μ	Bulk density, γ/(kN·m^{-3})
51.5	0.25	15.65
Cohesion, c/kPa	Internal friction angle, φ/(°)	Damping ratio, ξ
61.2	28.98	0.15

The element and the meshing are shown in Fig. 8.

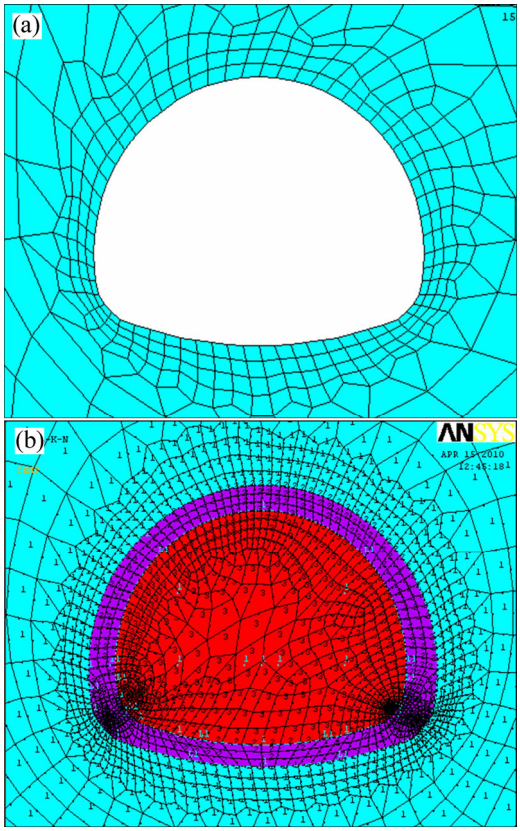

Fig. 8 Element and meshing: (a) Pseudo-static method and new method I; (b) New method II

5.2 Model and conclusion analysis

5.2.1 Pseudo-static strength reduction method

As known from Fig. 1, the soil shear strength parameter is continuously discounted until the instability damage occurs. Then, the structure safety factor of the tunnel under earthquake is obtained. Additionally, the critical strain figure and the safety factor under earthquake are obtained (shown in Fig. 9).

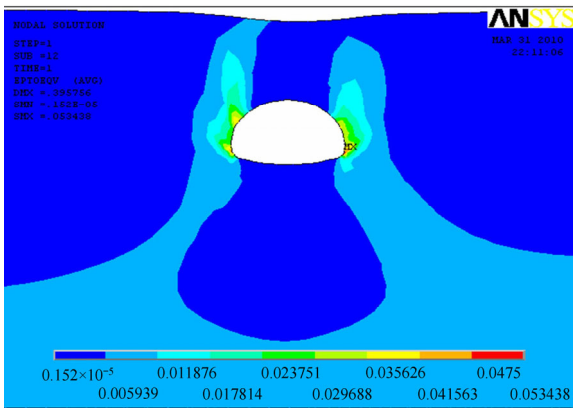

Fig. 9 Critical strain sketch nephogram (η=1.667)

As seen in Fig. 9 from the view of shear strength, the plastic zone of unlined soil tunnel first appears near the bottom corners.

5.2.2 New method I

As shown in Fig. 2, using the Block Lanczos modal analysis, the prior six frequencies of the tunnel structure are obtained (Table 2). The Rayleigh damping constants α and β are calculated by Eq. (2), namely, α=0.1528 and β=0.1008.

Table 2 Prior six-order frequencies f(Hz)

First frequency	Second frequency	Third frequency
0.6524	1.1969	1.4290
Fourth frequency	Fifth frequency	Sixth frequency
1.5452	1.8688	2.3254

Then, the El-Centro wave is input and the displacement time history curve of the upper right corner vertex A is obtained (shown in Fig. 10).

As seen in Fig. 10, the level displacement of vertical boundary node is the biggest when time t is between 1 and 2 s. The vertical boundary displacement at time T= 1.8 s can be extracted, as listed in Table 3.

From Fig. 1, the soil shear strength parameter is continuously discounted until the instability damage occurs and then the structure safety factor of the soil mass surrounding a tunnel under an earthquake is obtained. Additionally, the critical strain figure and safety factor under earthquake are obtained (shown in Fig. 11).

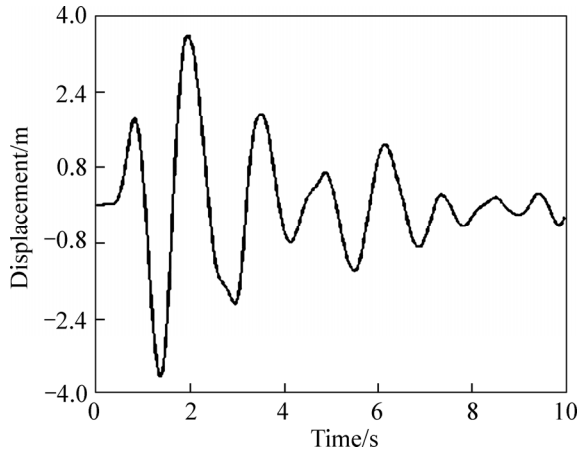

Fig. 10 Displacement time history of vertex A

Table 3 Horizontal node displacement of vertical boundary when T is 1.8 s/m

Node	Displacement/m	Node	Displacement/m
66	-0.36463×10^{-1}	110	-0.36465×10^{-1}
68	-0.22710×10^{-2}	175	-0.36220×10^{-1}
70	-0.45691×10^{-2}	177	-0.35763×10^{-1}
72	-0.68761×10^{-2}	179	-0.35104×10^{-1}
74	-0.91758×10^{-2}	181	-0.34256×10^{-1}
76	-0.11454×10^{-1}	183	-0.33231×10^{-1}
78	-0.13698×10^{-1}	185	-0.32039×10^{-1}
80	-0.15896×10^{-1}	187	-0.30694×10^{-1}
82	-0.18038×10^{-1}	189	-0.29210×10^{-1}
84	-0.20115×10^{-1}	191	-0.27599×10^{-1}
86	-0.22118×10^{-1}	193	-0.25873×10^{-1}
88	-0.24039×10^{-1}	195	-0.24045×10^{-1}
90	-0.25867×10^{-1}	197	-0.22125×10^{-1}
92	-0.27593×10^{-1}	199	-0.20121×10^{-1}
94	-0.29205×10^{-1}	201	-0.18044×10^{-1}
96	-0.30690×10^{-1}	203	-0.15902×10^{-1}
98	-0.32035×10^{-1}	205	-0.13704×10^{-1}
100	-0.33227×10^{-1}	207	-0.11460×10^{-1}
102	-0.34253×10^{-1}	209	-0.91816×10^{-2}
104	-0.35101×10^{-1}	211	-0.68811×10^{-2}
106	-0.35760×10^{-1}	213	-0.45730×10^{-2}
108	-0.36218×10^{-1}	215	-0.22735×10^{-2}

As seen in Fig. 11 from the view of shear strength, the plastic zone of unlined soil tunnel appears near the bottom corners.

5.2.3 New method II

As with new method I, taking α=0.1528, β=0.1008, as shown in Fig. 12, the horizontal support reactions F^{L}_{Rxi} and F^{R}_{Rxi} of the two lateral boundaries are obtained

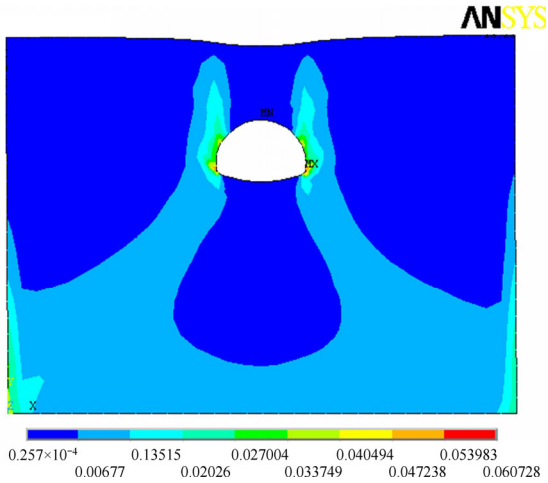

Fig. 11 Critical strain nephogram, η=1.6519

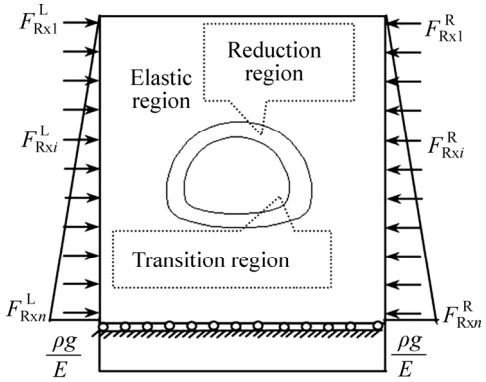

Fig. 12 Analysis model of dynamic finite element method

through static finite element analysis, which exert a driving force on the isolation body and the temperature of each node of the isolation body obtained from the heat analysis is put into the model.

Each node numbers on both the left and right lateral boundaries are shown in Fig. 13. The horizontal support reactions are listed in Table 4.

The thermal analysis reference temperature is 0 °C. The temperature difference obtained from Eq. (13) is about 0.0003 °C and the thermal boundary is shown in Fig. 14.

Based on the pseudo-static strength reduction method and the calculation results of new method I, the shear strength reduction zone thickness is 500 mm. By

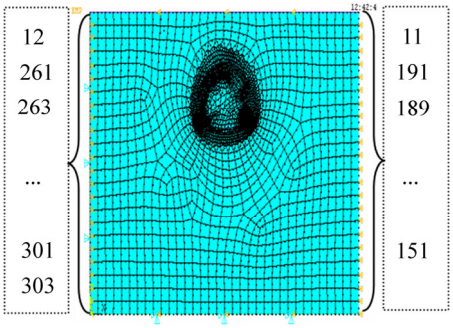

Fig. 13 Boundary node number

Table 4 Horizontal support reaction force along the vertical borders

Node	Force/N	Node	Force/N	Node	Force/N
11	2467.2	175	−59772	275	54835
12	−2466.1	177	−53995	277	60540
149	−130370	181	−40727	279	65798
151	−125440	183	−33241	281	70749
153	−128960	185	−25325	283	75547
155	−120900	187	−17163	285	80339
157	−106660	189	−8943.1	287	85249
159	−100660	191	−1591.1	289	90370
161	−94995	261	1593.0	291	95768
163	−89639	263	8943.8	293	101480
165	−84552	265	18363	295	107530
167	−79665	267	28302	297	113920
169	−74880	269	34317	299	120530
171	−70070	271	41730	301	125440
173	−65085	273	48580	303	130370

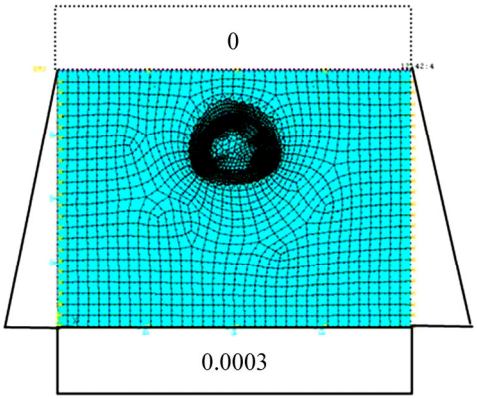

Fig. 14 Analysis model of thermal boundary

constantly discounting the shear strength parameters of the 500 mm thick layer of soil mass surrounding a tunnel, the critical strain nephogram and safety factor are shown in Fig. 15.

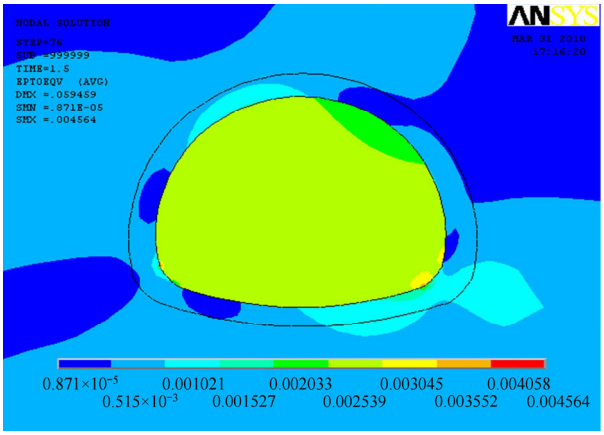

Fig. 15 Critical strain nephogram (η=1. 510)

6 Conclusions

1) Both of the two methods proposed are feasible.

2) For new method I, the load is obtained by the calculation of dynamic finite element. This method still uses the static evaluation method of the structure stability. However, the values of load are the results of dynamic calculations, and the dynamic performance of the tunnel is reflected, and the accuracy of the stability evaluation is improved to a certain extent.

3) For new method II, the load is a dynamic computation result but the stability method is no longer a static stability evaluation, and the stability evaluation method uses a dynamic calculation. This method can accurately evaluate the tunnel stability and the fracture surface of the tunnel as a response to earthquake ground motion can be directly obtained. The advantage of this method are that the load is obtained from the dynamic result, which can better reflect the dynamic performance of the rock mass or soil mass surrounding a tunnel.

4) Found from the strain figure, the plastic zone first appears near the bottom corners.

5) The safety factors of two new methods are much smaller than that of pseudo-static strength reduction method (1.667); the safety factor of new method II (1.6519) is smaller than that of new method I (1.510); but the difference is small, which proves that the methods suggested are feasible.

References

[1] SHI L. Loess tunnel seismic design study [D]. Xi'an: Chang'an University, 2005. (in Chinese)

[2] JIANG Q, FENG X T, XIANG T B. Discussion on method for calculating general safety factor of underground caverns based on strength reduction theory [J]. Rock and Soil Mechanics, 2009, 5(2): 291−296.

[3] LI S C, XU B S. Minimum safety factor method for stability analysis of surrounding rock mass of tunnel [J]. Rock and Soil Mechanics, 2007, 28(3): 549−554.

[4] YANG X L, HUANG F. Stability analysis of shallow tunnels subjected to seepage with strength reduction theory [J]. Journal of Central South University of Technology, 2009, 16(6): 1001−1005.

[5] STERPIL D, CIVIDINI A. A physical and numerical investigation on the stability of shallow tunnels in strain softening media [J]. Rock Mechanics and Rock Engineering, 2004, 37(4): 277−298.

[6] ZARETSKII Y K, KARABAEV M I, KHACHATURYAN N S. Construction monitoring of a shallow tunnel in the lefortovo district of moscow [J]. Soil Mechanics and Foundation Engineering, 2004, 41(2): 45−51.

[7] CHEN G X, ZHANG K X, XIE J F. A seismic performance analysis of the cave dwelling on the loess precipice [J]. Journal of Harbin University of Civil Engineering and Architecture, 1995, 28(1): 16−21.

[8] CHEN G X. Geotechnical earthquake engineering [M]. Beijing: Science Press, 2007: 30−100. (in Chinese)

[9] GAO F, REN X. Seismic response analysis of loess cave [J]. Journal

of Lanzhou Railway University: Natural Sciences, 2001, 20(3): 12−18.

[10] ZHENG Y R, ZHAO S Y, DENG C J. Development of finite element limit analysis method and its applications in geotechnical engineering [J]. Engineering Sciences, 2006, 8(12): 39−61.

[11] ZHENG Y R, CHEN Z Y, WANG G X. Engineering treatment of slope & landslide [M]. Beijing: China Communications Press, 2007: 20−150. (in Chinese)

[12] ZHENG Y R, QIU C Y, ZHANG H. Exploration stability analysis methods of surrounding rocks in soil tunnel [J]. Journal of Rock Mechanics and Engineering, 2008, 27(10): 254−260.

[13] QIU C Y, ZHENG Y R, SONG Y K. Exploring safety factors of unlined loess tunnel by ANSYS [J]. Journal of Underground Space and Engineering, 2009, 5(2): 291−296.

[14] YANG Z, ZHENG Y R, ZHANG H. Analysis on stability for the surrounding rock of tunnel and exploring the strength parameters [J]. Journal of Underground Space and Engineering, 2009, 5(2): 283−290.

[15] ZHANG H, ZHENG Y R, YANG Z. Exploration of safety factors of the loess tunnel [J]. Journal of Underground Space and Engineering, 2009, 5(2): 297−306.

[16] SHAN X L, SUN F. Analysis of seismic reliability of underground tunnel structure [J]. Journal of Natural Disasters, 2009, 18(2): 146−149.

[17] GU Z Q, PENG S Z, LI Z K. Underground tunnel engineering [M]. Beijing: Tsinghua University Press, 1994: 10−70. (in Chinese)

[18] CHEN L W, PENG J B, FAN W. Stability of loess hidden hole under earthquake [J]. Journal of Chang'an University: (Natural Science Edition), 2007, 27(6): 34−36.

[19] ZHANG L M, ZHENG Y R, WANG Z Q. Application of strength reduction finite element method to road tunnels [J]. Rock and Soil Mechanics, 2007, 28(1): 97−106.

(Edited by HE Yun-bin)